

# Droplet Coalescence and Freezing on Hydrophilic, Hydrophobic, and Biphilic Surfaces

Alexander S. Van Dyke<sup>1</sup>, Diane Collard<sup>2</sup>, Melanie M. Derby<sup>1</sup>, Amy Rachel Betz<sup>1\*</sup>

<sup>1</sup>Mechanical and Nuclear Engineering, Kansas State University, Manhattan, Kansas 66506, USA

<sup>2</sup>Chemical Engineering, Kansas State University, Manhattan, Kansas 66506, USA

## Abstract

Frost and ice formation can have severe negative consequences, such as aircraft safety and reliability. At atmospheric pressure, water heterogeneously condenses and then freezes at low temperatures. To alter this freezing process, this research examines the effects of biphilic surfaces (surfaces which combine hydrophilic and hydrophobic regions) on heterogeneous water nucleation, growth, and freezing. Silicon wafers were coated with a self-assembled monolayer and patterned to create biphilic surfaces. Samples were placed on a freezing stage in an environmental chamber at atmospheric pressure, at a temperature of 295 K, and relative humidities of 30%, 60%, and 75%. Biphilic surfaces had a significant effect on droplet dynamics and freezing behavior. The addition of biphilic patterns decreased the temperature required for freezing by 6 K. Biphilic surfaces also changed the size and number of droplets on a surface at freezing and delayed the time required for a surface to freeze. The main mechanism affecting freezing characteristics was the coalescence behavior.

Keywords: Biphilic, droplet coalescence, freezing, frost

On a cooled surface at atmospheric pressure, water first nucleates heterogeneously and subsequently, droplets may grow, coalesce, and freeze depending on the level of supercooling. Researchers have examined superhydrophobic [1-10], nano-engineered [7, 11, 12], and oil-impregnated surfaces [13, 14] to prevent frost or freezing by delaying nucleation, increasing droplet mobility, and reducing droplet contact area with the surface. Most research reports the total surface freezing time delay. Previous research that investigated direct condensation followed by freezing was performed at surface temperatures varying from 253 K – 268 K and relative humidities of 30 – 60% [2-4, 6, 9, 10]. This research examines the effects that biphilic surfaces (surfaces which combine hydrophilic and hydrophobic regions) have on heterogeneous water nucleation, droplet growth, and freezing behavior.

Biphilic surfaces [15-17] were fabricated on silicon wafers with a thermally grown oxide layer. Photolithography was used to mask the hydrophilic spots during a deposition of a self-assembled monolayer of Octadecyltrichlorosilane (OTS). The contact angle of the hydrophobic coating was measured to be 105°. Hydrophilic (Philic), hydrophobic (Phobic), and three types of biphilic surfaces (200IL, 200S, 25IL) were fabricated. The biphilic surfaces consisted of 25- $\mu$ m- or 200- $\mu$ m-hydrophilic circles on a hydrophobic background as shown in Figure 1. Before each experiment, the sample was cleaned with isopropyl alcohol and dried with nitrogen. After cleaning, the sample was placed on a freezing stage in an environmental chamber under quiescent flow conditions with a controlled air temperature (295 K) and relative humidity (RH). Each surface was tested at three relative humidities: 30%, 60%, and 75%. For each humidity and surface, the maximum freezing temperature was determined by incrementally decreasing the temperature of the freezing stage in approximately 0.5 K intervals. Once the surface reached a steady temperature, video was recorded for at least three hours at 35 $\times$  zoom to determine if freezing would occur. Freezing was detected by an index of refraction change; water droplets are clear whereas ice appears white. A surface was considered frozen when all individual droplets in the field of view had frozen. The visualization was performed by a Leica DVM2500 microscope with a maximum magnification of 2500 $\times$ .

Hydrophilic surfaces freeze closest to the freezing temperature of water, whereas hydrophobic surfaces can suppress freezing by a few degrees as shown in Figure 1. Biphilic surfaces can suppress

freezing temperatures to 6 K below the freezing temperature of water at a 60% RH. This appears to be a local optimum for which the droplet dynamics provide further insights. The size and distribution of the droplets at freezing were significantly different, even when freezing temperature was the same. On all surfaces, the first visible droplets were on the order of 5  $\mu\text{m}$ . This indicates that the variance in droplet size at freezing is due to different coalescence behavior, rather than nucleation. Further evidence that coalesce affects freezing was seen at surface temperatures where freezing did not occur. For example, on the 25IL surface at 60% RH and 268 K (one degree above the observed freezing temperature) droplets continued to coalesce and reached diameters up to 3 mm after 3 hours of observation. This coalesced droplet size is almost one order of magnitude greater than the average droplet diameter at freezing reported in Table 1.

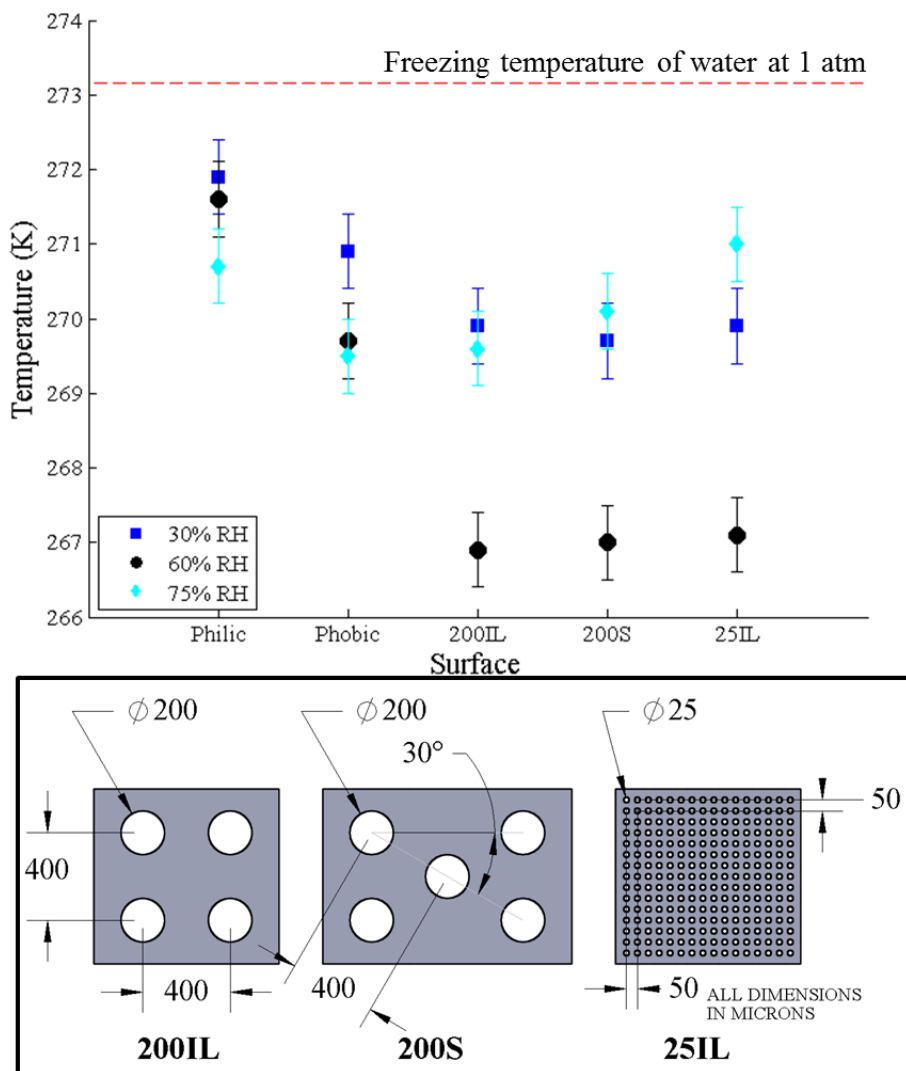
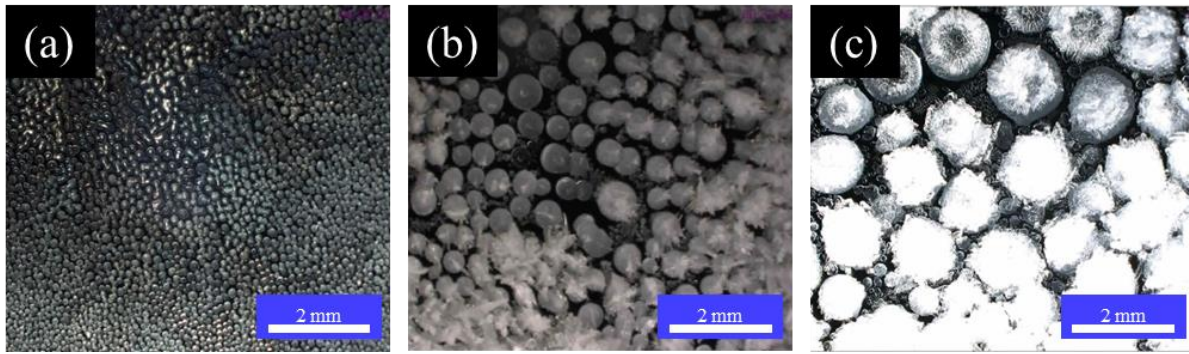
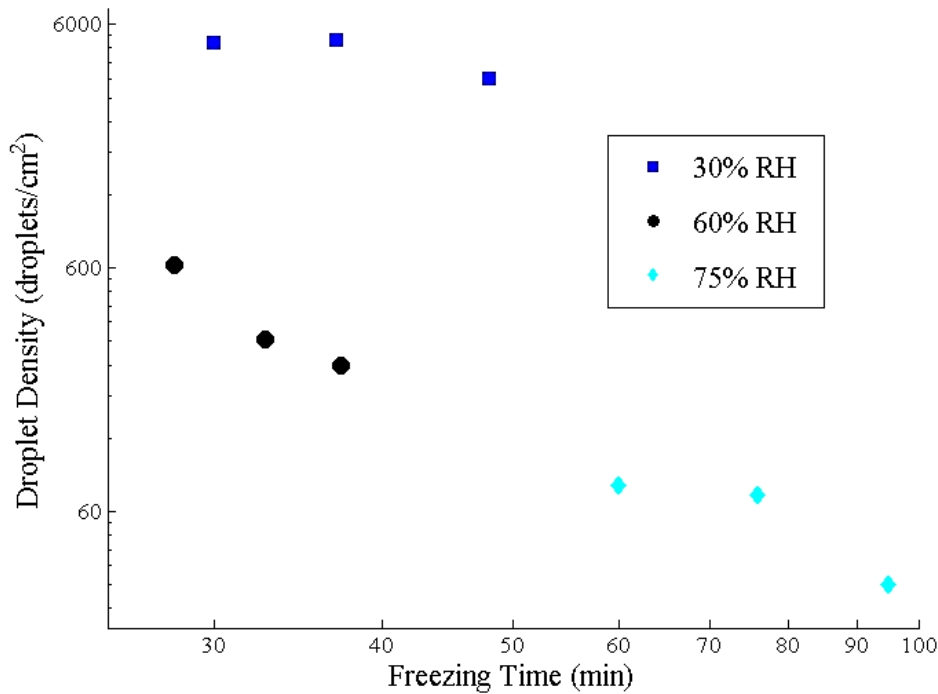


Figure 1. Maximum freezing (the highest temperature where freezing occurred) for all surfaces at three relative humidities (above). Schematic of biphilic surfaces tested (below).

In order to better understand the freezing behavior, droplet metrics were obtained at the maximum freezing temperature. The effects of relative humidity on droplet size and density after freezing are shown in Figure 2 and Table 1. Droplet density and size are not reported for the hydrophilic surface at 30% RH because the droplets merged and froze as a uniform sheet. As humidity increases, the density of droplets generally decreases, by up to two orders of magnitude. Subsequently, droplet size increases as humidity increases due to droplet coalescence. Table 1 shows the time required for each surface to freeze. The correlation between freezing time and droplet density for biphilic surfaces is plotted in Figure 3. For each relative humidity, longer freezing times were observed as droplet density decreased.



**Figure 2: Freezing point images on the 25IL surface for a) 30% b) 60% and c) 75% relative humidity at an air temperature of 295 K.**



**Figure 3. Droplet density versus freezing time for biphilic surfaces at the maximum freezing temperature. The atmospheric temperature was 295 K for all data points.**

Biphilic surfaces provide control over the coalescence dynamics. For example, at 60% and 75% RH, the 200IL surface significantly increases the time to freezing compared to the 200S surface. This aligns with a lower droplet density and a larger droplet diameter on the 200IL surface, thus demonstrating the importance of droplet coalescence on the freezing process. As droplets coalesce, energy is released (due to surface area reduction) and droplet volume increases (increasing the energy required for freezing). Assuming all droplets on hydrophobic and biphilic surfaces have a contact angle of  $105^\circ$  at freezing (Figure 4f), the average volume of a droplet at 60% RH can be estimated as 49, 75, 30, and 37 nL for the hydrophobic (Figure 4b), 200IL (Figure 4c), 200S (Figure 4d), and 25IL (Figure 4e) surfaces, respectively. Even though the 200IL and 200S surfaces share the same hydrophilic spot size, the estimated droplet volume on the 200IL surface is 150% greater than the 200S surface due to an increase in droplet coalescence, resulting in a nine minute increase in freezing time for the 200IL surface. The combination of coalescence and droplet growth delay freezing.

**Table 1. Freezing time, droplet density, and average diameter at freezing for all surfaces.**

Relative humidity	Surface	Freezing time (min:sec)	# of droplets per cm <sup>2</sup>	Average Drop diameter (mm)	STD of drop diameter (mm)
30%	Philic	13:00	N/A	N/A	N/A
	Phobic	56:00	1014 ± 60	0.33	0.142
	200IL	37:00	5123 ± 14	0.12	0.021
	200S	48:00	3598 ± 333	0.15	0.051
	25IL	30:00	4994 ± 414	0.14	0.033
60%	Philic	6:00	2807 ± 140	0.16	0.06
	Phobic	25:30	326 ± 10	0.55	0.153
	200IL	37:15	239 ± 14	0.57	0.131
	200S	28:00	618 ± 35	0.43	0.057
	25IL	32:45	305 ± 32	0.45	0.099
75%	Philic	25:00	67 ± 2	0.46	0.11
	Phobic	66:00	214 ± 32	0.35	0.119
	200IL	95:00	30 ± 2	0.90	0.194
	200S	60:00	77 ± 2	0.47	0.148
	25IL	76:00	70 ± 2	0.64	0.105

Due to the importance of droplet coalescence, further investigations were performed on the 25IL surface. As droplets began to coalesce on the 25IL surface at 75% RH, they were constrained by hydrophilic spots and an ordered pattern can be seen in Figure 5. Droplets nucleate on both the hydrophilic and hydrophobic regions. At first, droplets are randomly distributed but they begin to merge and are pinned to the hydrophilic spot. After a droplet has outgrown its hydrophilic spot, its contact angle is the same as the hydrophobic surface, as shown in Figure 4f. Biphilic surfaces do not have a strong impact on nucleation but change the coalescence behavior through this pinning mechanism. This sequence is observed throughout coalescence between growing and merging droplets.

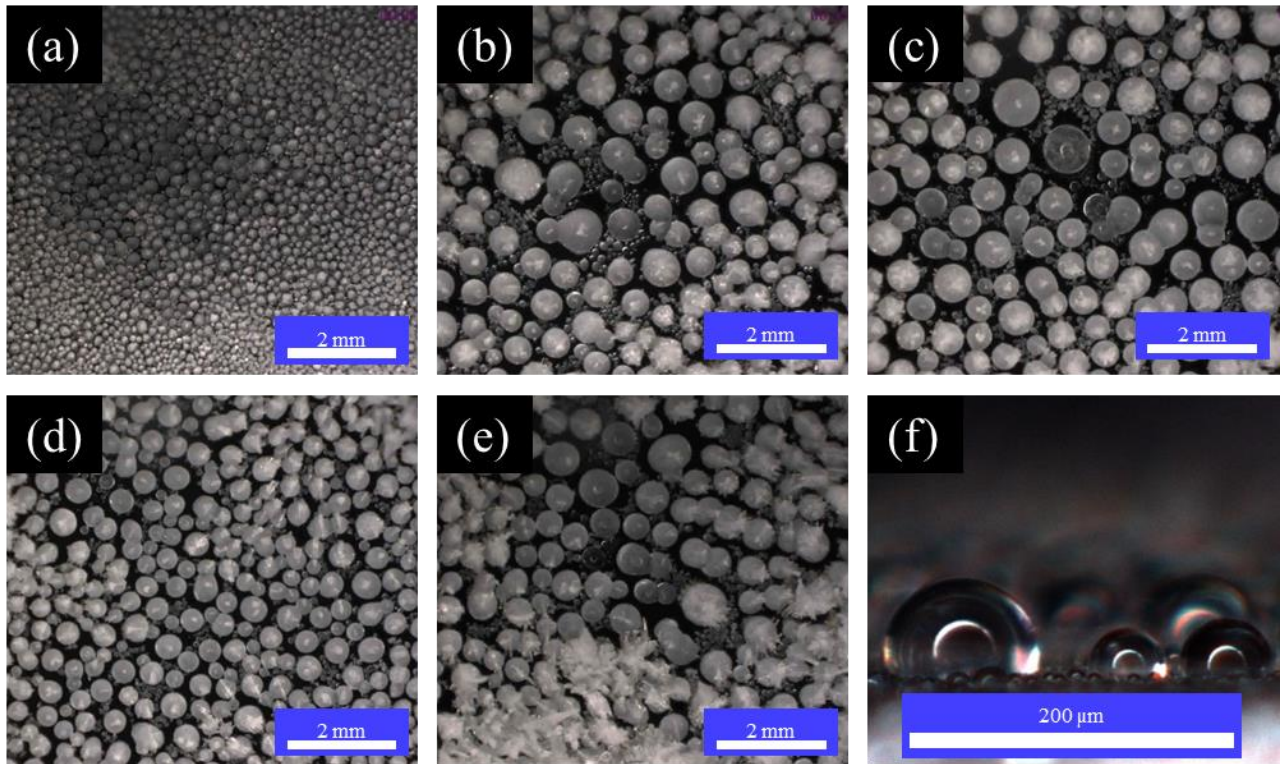


Figure 4. Freezing at 60% relative humidity for the a) hydrophilic, b) hydrophobic, c) 200IL, d) 200S, and e) 25IL surface. Image f is a side image of droplets on the 25IL surface.

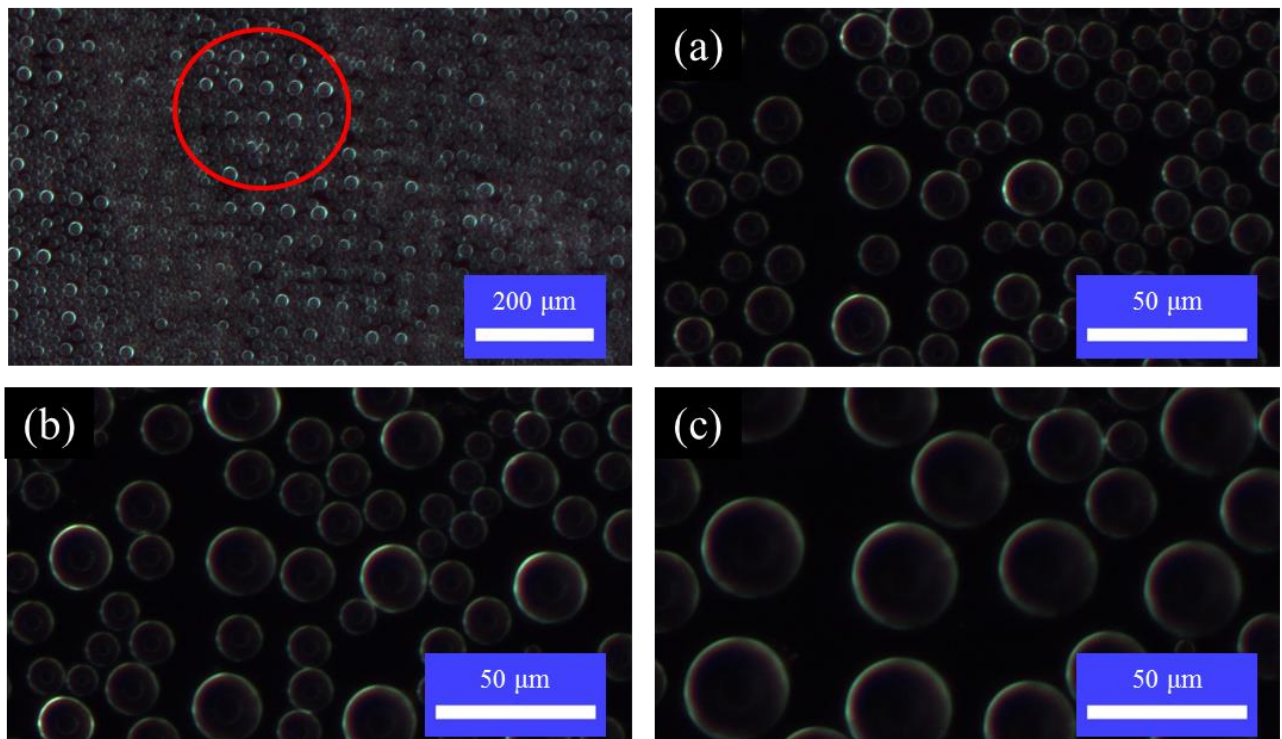


Figure 5. Droplet behavior, prior to freezing, on the 25IL surface at 75% RH. The top left figure shows the formation of an ordered pattern. Images 1-3 show the sequence of droplet growth and pinning behavior. The entire sequence occurred over a one minute span.

In conclusion, relative humidity, surface chemistry, and surface patterning significantly impact freezing temperature, droplet size and distribution, and the estimated droplet volume at freezing due to changes in coalescence. Coalescence dynamics are a critical factor affecting the freezing behavior.

## Acknowledgements

This material is based upon work supported by the National Science Foundation under Grant No. 1448270.

## References

- [1] S. Jung, M. Dorrestijn, D. Raps, A. Das, C. M. Megaridis and D. Poulikakos. Are superhydrophobic surfaces best for icephobicity? *Langmuir* 27(6), pp. 3059-3066. 2011.
- [2] L. Oberli, D. Caruso, C. Hall, M. Fabretto, P. Murphy and D. Evans. Condensation and freezing of droplets on superhydrophobic surfaces. *Adv. Colloid Interface Sci.* 210pp. 47-57. 2014. DOI: 10.1016/j.cis.2013.10.018.
- [3] J. B. Boreyko and C. P. Collier. Delayed frost growth on jumping-drop superhydrophobic surfaces. *ACS Nano* 7(2), pp. 1618-1627. 2013.
- [4] Q. Xu, J. Li, J. Tian, J. Zhu and X. Gao. Energy-effective frost-free coatings based on superhydrophobic aligned nanocones. *ACS Applied Materials and Interfaces* 6(12), pp. 8976-8980. 2014.
- [5] K. K. Varanasi, T. Deng, J. D. Smith, M. Hsu and N. Bhate. Frost formation and ice adhesion on superhydrophobic surfaces. *Appl. Phys. Lett.* 97(23), 2010.
- [6] Q. Hao, Y. Pang, Y. Zhao, J. Zhang, J. Feng and S. Yao. Mechanism of delayed frost growth on superhydrophobic surfaces with jumping condensates: More than interdrop freezing. *Langmuir* 30(51), pp. 15416-15422. 2014.
- [7] T. Maitra, M. K. Tiwari, C. Antonini, P. Schoch, S. Jung, P. Eberle and D. Poulikakos. On the nanoengineering of superhydrophobic and impalement resistant surface textures below the freezing temperature. *Nano Letters* 14(1), pp. 172-182. 2014.
- [8] L. Boinovich and A. M. Emelyanenko. Role of water vapor desublimation in the adhesion of an iced droplet to a superhydrophobic surface. *Langmuir* 30(42), pp. 12596-12601. 2014.
- [9] M. He, J. Wang, H. Li, X. Jin, J. Wang, B. Liu and Y. Song. Super-hydrophobic film retards frost formation. *Soft Matter* 6(11), pp. 2396-2399. 2010.
- [10] M. He, J. Wang, H. Li and Y. Song. Super-hydrophobic surfaces to condensed micro-droplets at temperatures below the freezing point retard ice/frost formation. *Soft Matter* 7(8), pp. 3993-4000. 2011. DOI: 10.1039/c0sm01504k.
- [11] T. M. Schutzius, S. Jung, T. Maitra, P. Eberle, C. Antonini, C. Stamatopoulos and D. Poulikakos. Physics of icing and rational design of surfaces with extraordinary icephobicity. *Langmuir* 31(17), pp. 4807-4821. 2015.
- [12] P. Eberle, M. K. Tiwari, T. Maitra and D. Poulikakos. Rational nanostructuring of surfaces for extraordinary icephobicity. *Nanoscale* 6(9), pp. 4874-4881. 2014.
- [13] S. B. Subramanyam, K. Rykaczewski and K. K. Varanasi. Ice adhesion on lubricant-impregnated textured surfaces. *Langmuir* 29(44), pp. 13414-13418. 2013.

- [14] K. Rykaczewski, S. Anand, S. B. Subramanyam and K. K. Varanasi. Mechanism of frost formation on lubricant-impregnated surfaces. *Langmuir* 29(17), pp. 5230-5238. 2013.
- [15] A. R. Betz, J. Jenkins, C. -. Kim and D. Attinger. Boiling heat transfer on superhydrophilic, superhydrophobic, and superbiphilic surfaces. *Int. J. Heat Mass Transfer* 57(2), pp. 733-741. 2013.
- [16] A. R. Betz, J. Xu, H. Qiu and D. Attinger. Do surfaces with mixed hydrophilic and hydrophobic areas enhance pool boiling? *Appl. Phys. Lett.* 97(14), 2010.
- [17] L. Zhai, M. C. Berg, F. Ç Cebeci, Y. Kim, J. M. Milwid, M. F. Rubner and R. E. Cohen. Patterned superhydrophobic surfaces: Toward a synthetic mimic of the namib desert beetle. *Nano Letters* 6(6), pp. 1213-1217. 2006.